Physics in Medicine and Biology

A new method for modelling the tongue-and-groove in treatment planning systems

To cite this article before publication: Victor Hernandez *et al* 2018 *Phys. Med. Biol.* in press https://doi.org/10.1088/1361-6560/aaf098

A new method for modelling the tongue-and-groove in treatment planning systems

V. Hernandez[1], Juan Antonio Vera-Sánchez[1], Laure Vieillevigne[2,3], C. Khamphan[4], Jordi Saez[5]

[1] Department of Medical Physics, Hospital Sant Joan de Reus, IISPV, 43201 Tarragona, Spain

[2] Department of Medical Physics, Institut Claudius Regaud - Institut Universitaire du Cancer de Toulouse, 31059 Toulouse, France

[3] Centre de Recherche et de Cancérologie de Toulouse, UMR1037 INSERM - Université Toulouse 3 – ERL5294 CNRS, Oncopole, 31037 Toulouse, France

[4] Medical Physics Unit, Institut Sainte Catherine, 84000 Avignon, France

[5] Department of Radiation Oncology, Hospital Clínic de Barcelona, 08036 Barcelona, Spain

Abstract

Commercial TPSs typically model the tongue-and-groove (TG) by extending the projections of the leaf sides by a certain constant width. However, this model may produce discrepancies of as much as 7–10% in the calculated average doses, especially for the High Definition multi-leaf collimator (MLC) (Hernandez *et al* 2017). The purpose of the present study is to introduce and validate a new method for modelling the TG that uses a non constant TG width. We provide the theoretical background and a detailed methodology to determine the optimal shape of this TG width from measurements and we fit an empirical function to the TG width that depended on two parameters a_1 and a_2. Parameter a_1 represents the TG width and a_2 introduces a curvature correction in the width near the leaf tip end. The new TG model was implemented in MATLAB and when the curvature correction was zero (a_2=0) it caused the same discrepancies as the constant width model used by the Eclipse TPS. On the other hand, when the experimentally determined a_2 was used the new model's calculations were in close agreement with measurements, with all differences in average doses <1%. Additionally, film dosimetry was used to successfully validate the potential of the new TG model to recreate the fine spatial details associated to TG effects. We also showed that the parameters a_1, a_2 depend solely on the MLC design by evaluating three different linear accelerators for each MLC model considered, namely Varian's High Definition and Millennium120 MLCs. In conclusion, a new method was presented that greatly improves the TG modelling. The present method can be easily implemented in commercial TPSs and has the potential to further increase their accuracy, especially for MLCs with rounded leaf ends.

1 Introduction

Intensity-modulated radiotherapy techniques require accurate modelling of the multi-leaf collimator (MLC) by treatment planning systems (TPS)(Li *et al* 2010; Mans *et al* 2016). Most MLC models have a 'tongue-and-groove' design in order to minimise the interleaf transmission (or leakage) between adjacent leaves. In this design, leaf sides are constructed with regions that extend outward (tongue) and inward (groove) in such a way that they interlock over a certain width with the complementary tongue and groove regions from the adjacent leaves. This arrangement diminishes interleaf transmission, but it also has the shortcoming of reducing the fluence whenever the leaf sides are exposed in the radiation beam. This effect is known as the tongue-and-groove (TG) effect (Deng *et al* 2001). In typical IMRT treatments, TG effects tend to be evenly distributed across the target volumes, but they can produce an underdosage of up to 5-7% in the average delivered doses if not properly taken into account (Lorenz *et al* 2008). As a consequence, it is crucial to adequately model the TG effect in TPSs (Yang *et al* 2016; Hillman *et al* 2018).

In a previous study we provided a set of tests for commissioning the TG modelling in TPSs and we reported limitations in the Eclipse TPS (Hernandez *et al* 2017). These limitations were notably significant for MLC test fields involving small dynamic MLC gaps, remarkably for the Varian High Definition MLC (HDMLC). In particular, discrepancies of up to 10% and 7% were found between calculated and average measured doses for test fields incorporating large TG effects with 5 and 10 mm gaps, respectively. These results were obtained for the Eclipse TPS, but most commercial TPSs use similar models and are therefore expected to yield similar results (Bedford *et al* 2013; Chen *et al* 2015; Yang *et al* 2016; Roche *et al* 2018).

The aims of the present study are twofold: (1) to introduce and validate a new tongue-and-groove model that improves the accuracy of dose calculations and (2) to provide a comprehensive methodology to derive the parameters used in the model.

2 Models and design of the experiments

2.1 Description of the MLC model

In the present study, an MLC model taking into account rounded leaf ends, MLC transmission and a new tongue-and-groove model was implemented. Similarly to the Eclipse TPS, leaf edges were modelled as straight and the transmission through rounded leaf ends was accounted for by computing the fluence after shifting the leaf positions by a certain leaf offset. Thus, leaves were pulled back so that the gap for all leaf pairs was increased by twice this leaf offset value, which is defined as the dosimetric leaf gap (DLG) parameter. Hence, the fluence for a completely closed pair of leaves was computed as the fluence produced by a gap equal to the DLG parameter. Both interleaf and intraleaf transmission (T_{inter} and T_{intra}, respectively) were modelled. The value of T_{inter} was

empirically selected and T_{intra} was set to keep the mean transmission (T_{mean}) equal to the measured average transmission introduced into the Eclipse TPS. Zero transmission was considered for the jaws.

The tongue-and-groove design is illustrated in Fig. 1. When a leaf side is exposed, its protruding part extends beyond its nominal position, additionally shielding part of the beam. To model the fluence reduction caused by this design, the projections of the leaf sides are typically extended a constant width in the direction perpendicular to the leaf motion (Varian Medical Systems 2015; Chen *et al* 2015).

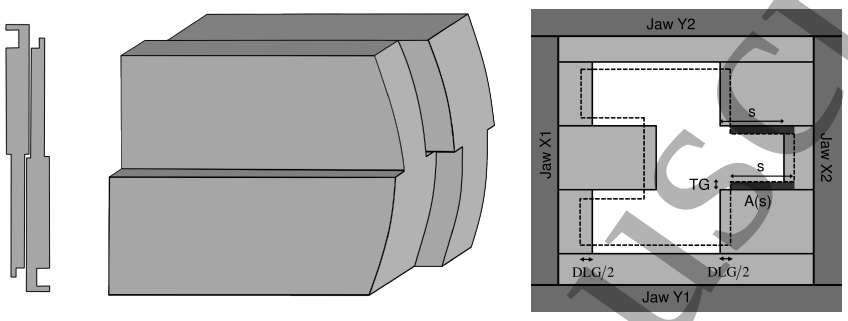

Figure 1: A sketch of the frontal section of two adjacent leaves is presented in (a) to show the interlock between complementary tongue and groove regions. A 3D view with two adjacent leaves is illustrated in (b) showing the rounded leaf ends and the tongue-and-groove design. In (c), an example with three pairs of leaves (in light grey) is shown along with the corresponding fluence aperture used for dose calculations (dashed lines) after taking into account the dosimetric leaf gap (DLG) and the tongue-and-groove (TG) effect. Proportions are not to scale and are for demonstration purposes only.

As a consequence, in this simplified model the fluence map in the direction of leaf motion is increased by the DLG (each leaf tip being pulled back DLG/2), while in the perpendicular direction it is reduced by a certain width at each leaf side. The difference between the nominal leaf edges and the fluence map used for dose calculations is shown in Fig. 1(c). This MLC model is quite simple and involves very few parameters: the DLG, interleaf and intraleaf transmissions and a certain tongue width.

2.2 New tongue-and-groove model

We hypothesised that the TG could be better modelled by subtracting a non-uniform width from the fluence map instead of subtracting a constant width. To obtain the optimal shape of the non-uniform TG width, a generic TG width was first assumed and simplified theoretical expressions were derived for determining the optimal shape of the TG width from measurements.

Let us first consider the dose produced by a generic sweeping MLC gap with a

constant gap size, D_{SG}. D_{SG} is proportional to the exposed area of the leaf pair ($\mathrm{A}_{\mathrm{leaf\ pair}}$) and the MLC transmission and can be expressed as

$$D_{SG} = D_{\mathrm{open}}\, T_{\mathrm{eff}} + k\, A_{\mathrm{leaf\,pair}}\ , \tag{1}$$

where D_{open} is the dose delivered by the open field (i.e., with the same jaw setting and without MLC) and T_{eff} is the effective MLC transmission. T_{eff} is defined as a function of the mean MLC transmission T_{mean} and the distance d travelled by the MLC gap (assuming $d >>$ Gap) as

$$T_{\mathrm{eff}} = T_{\mathrm{mean}}\, \frac{(d - \mathrm{Gap})}{d}\ . \tag{2}$$

In the sweeping gap fields without TG ($\mathrm{SG}_{\mathrm{TG0}}$) used to measure the DLG parameter

$$A_{\mathrm{leaf\,pair}} = \mathrm{w}_{\mathrm{leaf}}\, \mathrm{Gap}_{\mathrm{eff}}\ , \tag{3}$$

where $\mathrm{w}_{\mathrm{leaf}}$ is the leaf width and the effective gap is defined as

$$\mathrm{Gap}_{\mathrm{eff}} = \mathrm{Gap} + \mathrm{DLG}\ . \tag{4}$$

Hence, for sweeping gap fields without TG Eq. (1) results into

$$D_{\mathrm{SG_{TG0}}} = D_{\mathrm{open}}\, T_{\mathrm{eff}} + k\, \mathrm{w}_{\mathrm{leaf}}\, \mathrm{Gap}_{\mathrm{eff}}\ . \tag{5}$$

Since $\mathrm{w}_{\mathrm{leaf}}$ is constant for all leaves of the same type, it can be absorbed into a new constant k_2=$k\,\mathrm{w}_{\mathrm{leaf}}$ and the expression used to determine the DLG (LoSasso *et al* 1998; Mei *et al* 2011) is obtained where the quantity $D = D_{\mathrm{SG_{TG0}}}$-$D_{\mathrm{open}}T_{\mathrm{eff}}$ can be plotted as a function of the gap. The parameter DLG can the be derived as the negative gap necessary to produce a quantity D equal to zero:

$$D = D_{\mathrm{SG_{TG0}}} - D_{\mathrm{open}}\, T_{\mathrm{eff}} = k_2\ (\mathrm{Gap} + \mathrm{DLG})\ . \tag{6}$$

In clinical cases, however, adjacent leaves differ in their positions and the dose produced by sweeping gaps is affected by the TG effect. To investigate this effect let us compute the dose produced by an asynchronous sweeping gap test (aSG) with a constant difference s between adjacent leaf positions. In this test all leaf pairs produce the same gap (as in Fig. 1(c)), but it incorporates the TG effect due to the difference in the positions between neighbour leaves. All leaves move at the same constant speed and travel the same distance, d, keeping the shape of the MLC pattern unchanged. A more detailed description of this test can be found in our previous publication (Hernandez *et al* 2017). To account for the TG effect, a certain area $A(s)$ can be subtracted from

the fluence map at each leaf side. $A(s)$ depends on the difference between adjacent leaf positions, s, and is shown in Fig. 1(c) (see rectangle in dark grey). The dose for this field D_{aSG} can be obtained from Eq. (1) with an exposed area of the leaf pair given by

$$A_{\mathrm{leaf\,pair}} = \mathrm{w}_{\mathrm{leaf}}\,\mathrm{Gap}_{\mathrm{eff}} - 2\,A(s)\ . \tag{7}$$

Taking into account that the constant k can be obtained from the sweeping gap test without TG ($D_{\mathrm{SG_{TG0}}}$) provided in Eq. (5), the dose D_{aSG} can be written as

$$D_{\mathrm{aSG}}(s) = D_{\mathrm{SG_{TG0}}} - 2\,\frac{D_{\mathrm{SG_{TG0}}} - D_{\mathrm{open}}\,T_{\mathrm{eff}}}{\mathrm{w}_{\mathrm{leaf}}\,\mathrm{Gap}_{\mathrm{eff}}} A(s)\ . \tag{8}$$

$A(s)$ can then be isolated from Eq. (8) as

$$A(s) = \frac{D_{\mathrm{SG_{TG0}}} - D_{\mathrm{aSG}}(s)}{D_{\mathrm{SG_{TG0}}} - D_{\mathrm{open}}\,T_{\mathrm{mean}}\,(\frac{d-\mathrm{Gap}}{d})} \left(\frac{(\mathrm{Gap}+\mathrm{DLG})\mathrm{w}_{\mathrm{leaf}}}{2}\right)\ . \tag{9}$$

Thus, if the dose for the aSG tests D_{aSG} is measured for a series of s values, $A(s)$ can be obtained for each s using Eq. (9). For s values smaller than the leaf gap (i.e., no interdigitation between leaves from opposed MLC banks), $A(s)$ is equal to the area of the optimal TG profile from zero to s. Hence, once the curve $A(s)$ is determined, the width of the TG profile $\mathrm{w}(s)$ can be obtained as the first derivative of $A(s)$:

$$\mathrm{w}(s) = \frac{dA(s)}{ds}\ . \tag{10}$$

In the previous expressions we assumed that the area $A(s)$ was 'subtracted' from the fluence map, but certain fluence might be assigned to that region to account for MLC transmission through the TG width. If a transmission value T' was assigned to the TG profile the previous method and equations would still be valid, but both $A(s)$ and $\mathrm{w}(s)$ in Eq. (9) and Eq. (10) should then be increased by a factor $1/(1\text{-}T')$ in order to produce the same effective reduction.

The fluence below the TG width can be computed as

$$\mathrm{Fluence} = \frac{\mathrm{pixel\ size} - \mathrm{w}(s)}{\mathrm{pixel\ size}}\ , \tag{11}$$

where a pixel size greater than the TG width was assumed for simplicity. Otherwise the TG width encompasses several pixel rows and proper sampling is necessary (Yang *et al* 2016).

2.3 Calculation algorithm and implementation of the model

To validate the model, in-house software for computing beam fluences was developed in MATLAB® (Mathworks, Massachusetts, USA), implementing the new TG model with a variable TG width. The resolution used in the fluence map was 0.3125 mm (measured at the isocenter plane) in both directions. This value was selected because it is the same resolution that recent versions of the Eclipse TPS use in fluence maps (Torsti *et al* 2013) and we considered it interesting to investigate whether it was sufficient to characterise the spatial variations produced by the TG effect. Additionally, with this resolution all leaf widths of current Varian MLCs (2.5 mm, 5 mm and 10 mm) are multiples of the pixel size, which simplifies the calculations. Indeed, the thinner leaves of the HD120 MLC (2.5 mm wide) comprise 8 pixel rows in the fluence map, while leaves 5 mm and 10 mm-wide comprise 16 and 32 pixel rows, respectively.

The software reads all the information from the DICOM plan as exported from the TPS and computes the fluence for all the beams, as previously described. Thus, leaves were pulled back DLG/2 to account for rounded leaf ends and the TG effect was modelled by extending the leaf sides considering the optimal width obtained with Eq. (10). After that, the fluence was set to 1 in pixels fully included in the beam, while in regions shielded by the MLC it was set to the a different transmission value depending on the location of the pixels: T_{inter} in the first and last row of pixels corresponding to each leaf and T_{intra} in the central rows.

In beams with a dynamic MLC the leaves move between control points at a constant speed and a meterset weight is used to define the fraction of monitor units (MU) delivered between each pair of control points. In that case the computation of the fluence was divided into two steps. Firstly, the fluence was calculated for each pair of control points taking into account the meterset fraction during which each pixel was exposed. Secondly, the overall fluence for the beam was obtained by summation of the fluence between all the control points in the beam (Chui *et al* 2003). In this study only beams with static gantry were evaluated, but the code can be easily used in arc therapy by dividing the arcs into multiple static fields with different gantry angles and computing a partial fluence for each of them.

In fluence-based TPSs, the fluence is computed for each beam and a dose deposition engine subsequently calculates the dose distribution based on the computed beam fluences. In this study, the fluence map was convolved with a kernel optimised at 10 cm depth in order to compare calculations with measurements. The algorithm described by Azcona and Burguete 2010 was used to obtain the dose maps from the computed fluence maps. The kernel parameters were obtained following the procedure described by Tillikainen *et al* 2007 and the kernel was sampled with the same spatial resolution as the fluence maps. The fluence energy map was first calculated from the fluence of every beam by taking into account the deviations from a flat distribution due to lateral energy fluence variations. Next, the fluence energy map was convolved with the kernel. Finally, the dose map was computed by multiplying the former convolution by the reference dose at the working depth and by the number of monitor units delivered by the beam. To determine the average dose delivered by the aSG tests the calculated

doses were averaged over 20 mm in the direction perpendicular to the leaf motion, thus including several leaves and smoothing out the spatial variations associated to the TG effect.

2.4 Equipment and experiments

Four institutions participated in the study and six Varian linear accelerators (linacs) were evaluated: three linacs equipped with a High Definition HD120 MLC (HDMLC) and three linacs with a Millennium120 MLC. The four institutions used the Eclipse TPS and TPS calculations were included in this study for comparison purposes. Both the Analytical Anisotropic Algorithm and AcurosXB dose calculation algorithms were evaluated, but we already showed that they produced equivalent results in these tests (Hernandez *et al* 2017). All TPS calculations were carried out at the 1 mm grid size, which is the finest grid allowed by the system. The various linacs, MLCs and TPSs used are detailed in Table 1.

Table 1: Summary of the equipment used

Centre	Linac	MLC model	TPS version
A	Trilogy^{TM}	HDMLC	Eclipse 13.5
A	2300iX	Millennium120	Eclipse 13.5
B	TrueBeam STx	HDMLC	Eclipse 13.5 & 15.5
B	TrueBeam	Millennium120	Eclipse 13.5 & 15.5
C	TrueBeam STx	HDMLC	Eclipse 13.7
D	2100CD	Millennium120	Eclipse 13.7

The model was validated by evaluating the accuracy of the calculated average doses for the aSG tests and of the calculated dose distributions. Measurements of the average dose were carried out using a PTW Farmer-type ionisation chamber model 30013 positioned perpendicular to the MLC movement direction. A Farmer-type chamber was selected because its active length (23 mm) encompasses several leaves, providing a good estimate of the average impact of the TG effect. Gap sizes of 5, 10, 20 and 30 mm were evaluated. For each of these gap sizes the range of distances between adjacent leaves (s values) was 0–10 mm, 0–14 mm, 0–30 mm and 0–30 mm, respectively. Measurements were made in water at the isocentre, at 10 cm depth and with x-rays with a nominal energy of 6 MV. For comparison purposes additional measurements were also carried out in different conditions and with 18 MV photon beams.

Finally, to investigate if our calculations could replicate the spatial distribution of the TG effect, radiochromic EBT3 films (ISP, Wayne, NJ) were exposed at the isocentre at 10 cm depth for the aSG tests with s values equal to 0, 'gap/2' or 'gap' for the 10 and 20 mm gaps. An Epson 10000XL scanner (Seiko EPSON Corp., Nagano, Japan) was used for digitation of the radiochromic film. The efficient protocol by Lewis et al (2012) and the methodology proposed by Vera Sanchez et al (2016) were followed.

3 Results

3.1 New tongue-and-groove model

Average doses for the aSG tests were measured with the Farmer chamber for the various gap sizes and s values. For all fields with $s <$ gap (i.e., without interdigitation) $A(s)$ was calculated from the measured D_{aSG} values by using Eq. (9). The $A(s)$ values obtained with different gap sizes were comparable, which shows that the $A(s)$ curve can be used regardless of the gap size (see Fig. 2(a)). Moreover, linacs with the same MLC model produced similar $A(s)$ values, with maximum differences $< 0.1\,\mathrm{mm}^2$ (see Fig. 2(b)). Hence, $A(s)$ curves from the same MLC model were averaged and an analytic function was fitted to the average curve. Since the curves were approximately linear for $s > 5\,\mathrm{mm}$ the following linear fit with an exponential correction was used:

$$A(s) = a_1.s - a_2\left(1 - e^{-a_3.s}\right) . \tag{12}$$

Since the TG width should start at zero, the three parameters in Eq. (12) are not independent and the following condition can be imposed

$$\left.\frac{dA(s)}{ds}\right|_{s=0} = 0 \quad \Longrightarrow \quad a_3 = \frac{a_1}{a_2} \tag{13}$$

and, consequently,

$$A(s) = a_1.s - a_2\left(1 - e^{-a_1/a_2.s}\right) . \tag{14}$$

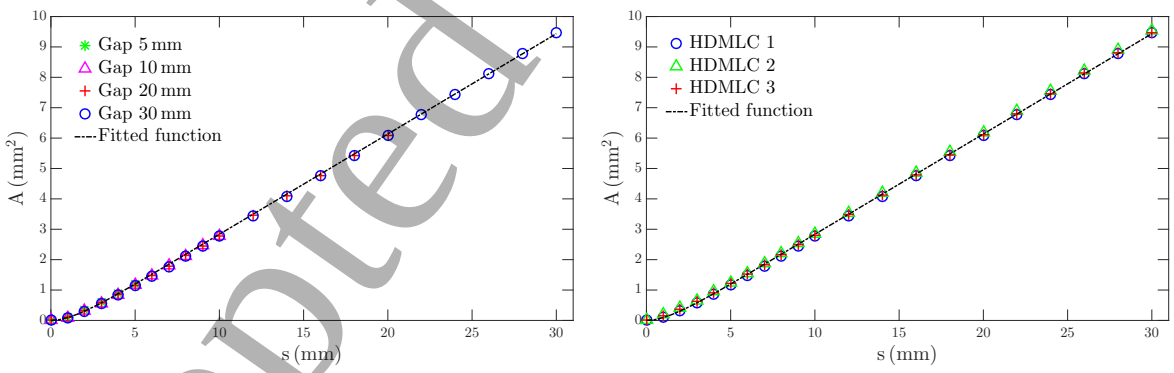

(a) (b)

Figure 2: Tongue-and-groove area $A(s)$ as a function of the shift s between adjacent leaf positions for the High Definition MLC (HDMLC) and the corresponding fitted function. Data obtained with different MLC gap sizes for a particular MLC is given in (a). In (b) the data from different linacs with the HDMLC are presented.

As can be seen in Fig. 2, Eq. (14) provided a good fit, with differences with respect to average $A(s)$ values $<0.05\,\mathrm{mm}^2$. The TG width can then be obtained with Eq. (10) and results into

$$\mathrm{w}(s) = a_1 \left(1 - e^{-a_1/a_2 . s}\right) \ . \tag{15}$$

Distinctive $A(s)$ curves were obtained for each MLC model (HDMLC and Millennium120) and are presented in Fig. 3(a). The fitting parameters were $a_1 = 0.330 \pm 0.001$ mm, $a_2 = 0.465 \pm 0.016\,\mathrm{mm}^2$ for the HDMLC and $a_1 = 0.331 \pm 0.001$ mm, $a_2 = 0.838 \pm 0.027\,\mathrm{mm}^2$ for the Millennium120 MLC. According to its beam calculation report, Eclipse v15 assumes a constant TG width of 0.33 mm, which is equivalent to considering a linear $A(s)$ curve with a constant slope of 0.33 mm. This curve is also shown in Fig. 3(a) to illustrate the differences between the models.

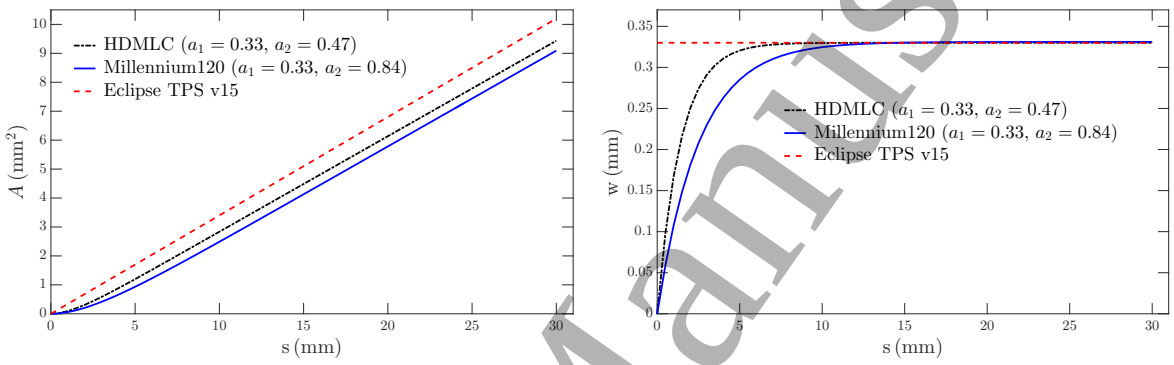

(a) (b)

Figure 3: Average fitted curves to the tongue-and-groove area $A(s)$ for the two MLC models are shown in (a). The corresponding shapes of the tongue-and-groove width are given in (b).

The shapes of the optimal TG width obtained with Eq. (15) are illustrated in Fig. 3(b) and, as can be seen, they differed from the constant tongue width assumed by the Eclipse TPS. Indeed, the profile considered by the Eclipse TPS clearly overestimated the TG width near the leaf tip (i.e., for small s values), underestimating the fluence in that region and the corresponding delivered dose.

3.2 Validation of the model (1): average doses

In this section, the average doses produced by asynchronous sweeping gap tests are evaluated. Calculations with the new model were compared to average doses measured with the Farmer chamber and to calculations with the Eclipse TPS. The specific DLG and average MLC transmission values from each accelerator were considered in the calculations. For all the accelerators with the same MLC model the same parameters a_1 and a_2 were used for modelling the TG. Regarding the modelling of MLC transmission,

the calculated average doses only depended on the average MLC transmission and were not affected by the interleaf transmission parameter.

Figure 4 shows the measured and calculated average doses with gap sizes of 10 mm and 20 mm for a representative case of each MLC model. Calculations from the Eclipse TPS version 13 (for both MLC models) were accurately reproduced with the new TG model when the parameters $a_1 = 0.37$ mm and $a_2 = 0$ were used, which is equivalent to considering a constant TG width of 0.37 mm. Calculations from Eclipse v15 were reproduced with $a_1 = 0.33$ mm, which agrees with the value reported by the manufacturer.

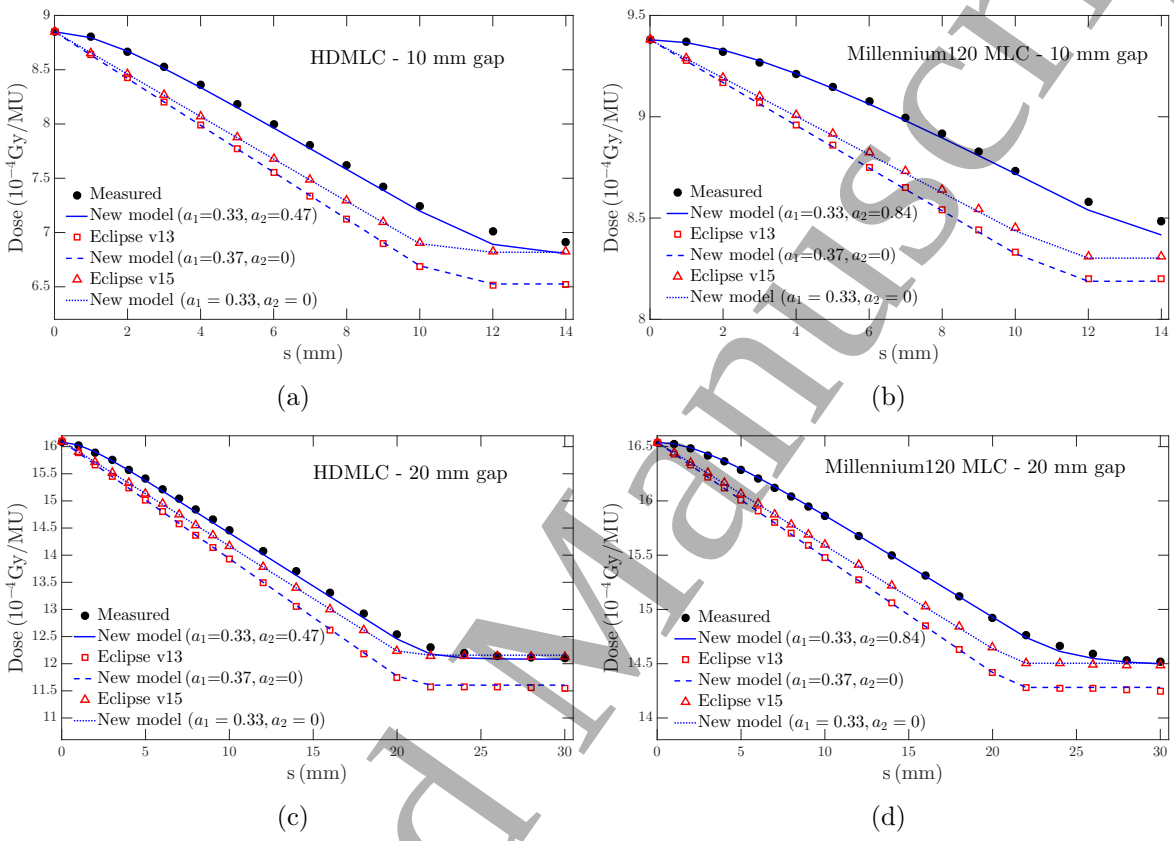

Figure 4: Measured and calculated average doses produced by asynchronous sweeping gap tests with different shifts s between adjacent leaf positions. The data corresponds to gap sizes of 10 mm (upper) and 20 mm (lower) for a representative case of each MLC model.

On the other hand, an excellent agreement between calculations and measurements was obtained using the new TG model with the a_1, a_2 parameters determined from the experimental $A(s)$ curves. In general, slightly higher deviations were found when the difference between adjacent leaf positions exceeded the leaf gap, with differences up to 2% for the 5 mm gaps. In that case interdigitation between leaves from opposed banks takes place, which might require a better modelling of other aspects such as rounded leaf ends and leaf transmission. However, the focus of this study is the TG effect, therefore results from leaf interdigitation will hereafter be excluded.

Differences of as high as 10% and 7% were obtained with Eclipse v13 for the HDMLC and the Millennium MLC, respectively, as previously reported (Hernandez *et al* 2017). Eclipse v15 yielded better results, with differences of around 6.5% for the 5 mm gap and 4.5% for the 10 mm gap and the HDMLC. These discrepancies in the average doses between calculations and measurements are illustrated in Fig. 5 for the HDMLC and the Millenium120 MLC (for the new model and for Eclipse v15). As can be seen, when the new TG model was used all differences were within ±1%.

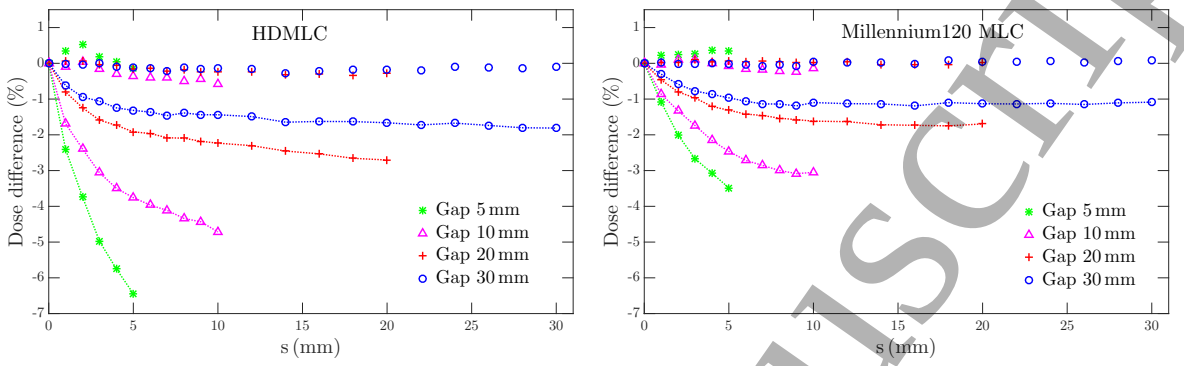

(a) (b)

Figure 5: Differences between measured and calculated average doses produced by asynchronous sweeping gaps of different gap sizes and different shifts s between adjacent leaf positions. Symbols without lines indicate results with the new model and symbols with dotted lines indicate results from Eclipse v15 for the (a) HDMLC and the (b) Millennium120 MLC.

These results were obtained for photon beams with a nominal energy of 6 MV at 10 cm depth in water. However, measurements were also carried out at other depths (1.5 cm and 20 cm) and very similar results were found. For comparison purposes, the tests were also carried out with 18 MV photon beams and, considering the same set of configuration parameters a_1 and a_2, deviations between calculations and measurements remained within ± 1.5%.

Finally, the maximum accuracy achievable with the constant width model was investigated. To that aim, the calculations for the asynchronous sweeping gap tests were repeated varying the width (a_1 parameter) from zero to 0.5 mm in 0.01 mm steps. Next, for each a_1 value and each gap size the maximum percentage dose difference (for any s) was obtained and plotted as a function of a_1. As shown in Fig. 6, the optimal TG width (a_1 parameter) for the constant width model depends on the gap size. The optimal value seems to be in the 0.28–0.32 mm range, but any particular value of a_1 will cause discrepancies >2–3% in the average doses produced by some gap sizes, or even larger if a wider range of gap sizes was considered.

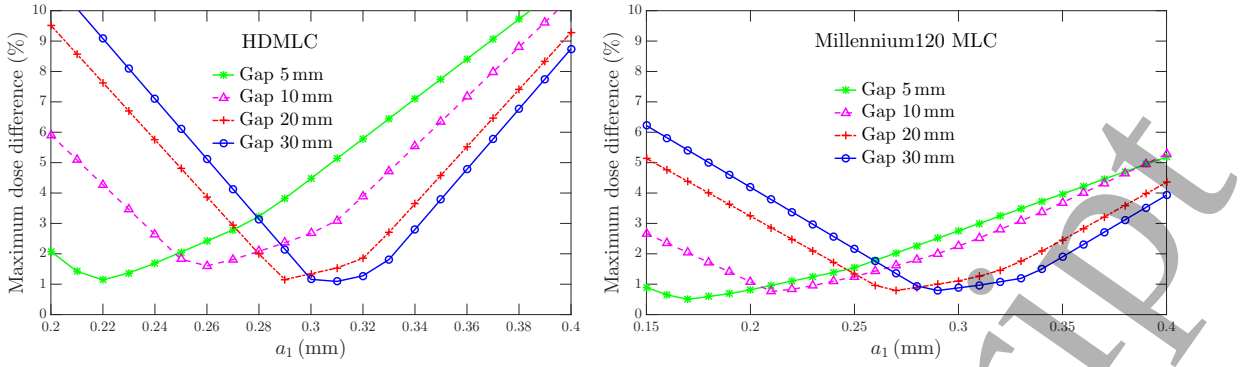

(a) (b)

Figure 6: Maximum differences for any s value between measurements of asynchronous sweeping gaps and calculations with the constant width model (a_2=0) as a function of the TG width a_1 for the (a) High Definition MLC and (b) the Millennium120 MLC.

3.3 Validation of the model (2): film dosimetry

In this section the ability of our new model to reproduce the fine details associated to the TG effect is investigated. To that aim, the dose profiles in the direction perpendicular to the leaf motion obtained for asynchronous sweeping gap tests were measured with film dosimetry and compared to calculated profiles.

The interleaf transmission parameter T_{inter} was selected empirically in order to maximise the agreement between calculated and measured profiles for sweeping gaps without TG (i.e., $s = 0$). The measured T_{mean} and the obtained T_{inter} values were 0.0125, 0.025 for the HDMLC and 0.015, 0.03 for the Millennium 120 MLC, respectively. However, these values depend on the resolution (i.e, the pixel size) used and are not to be considered universal.

The calculated and measured profiles for gaps of 10 mm and 20 mm and different amounts of TG effect are given in Fig. 7. A close agreement was found in the spatial distribution, which shows that the new model can correctly replicate even the fine details produced by the TG effect.

The dose peaks in the profiles without TG (s=0) are due to the increased transmission between the leaves (T_{inter}). As shown in Fig. 7(a), the average dose was slightly higher in the central region of the profile (y < 4 cm). This is due to the fact that central leaves are thinner, and the higher frequency of interleaf transmissions in this region produces a higher effective MLC transmission. This spatial dependence of the MLC transmission was intrinsically taken into account in the model by considering different values for T_{inter} and T_{intra}.

In the profiles with $s =$ 'gap/2' and $s =$ 'gap' there were dose dips due to the TG effect, which also reduced the average dose, especially in the central region. Our model was able to accurately calculate both the average dose reduction and the spatial distribution

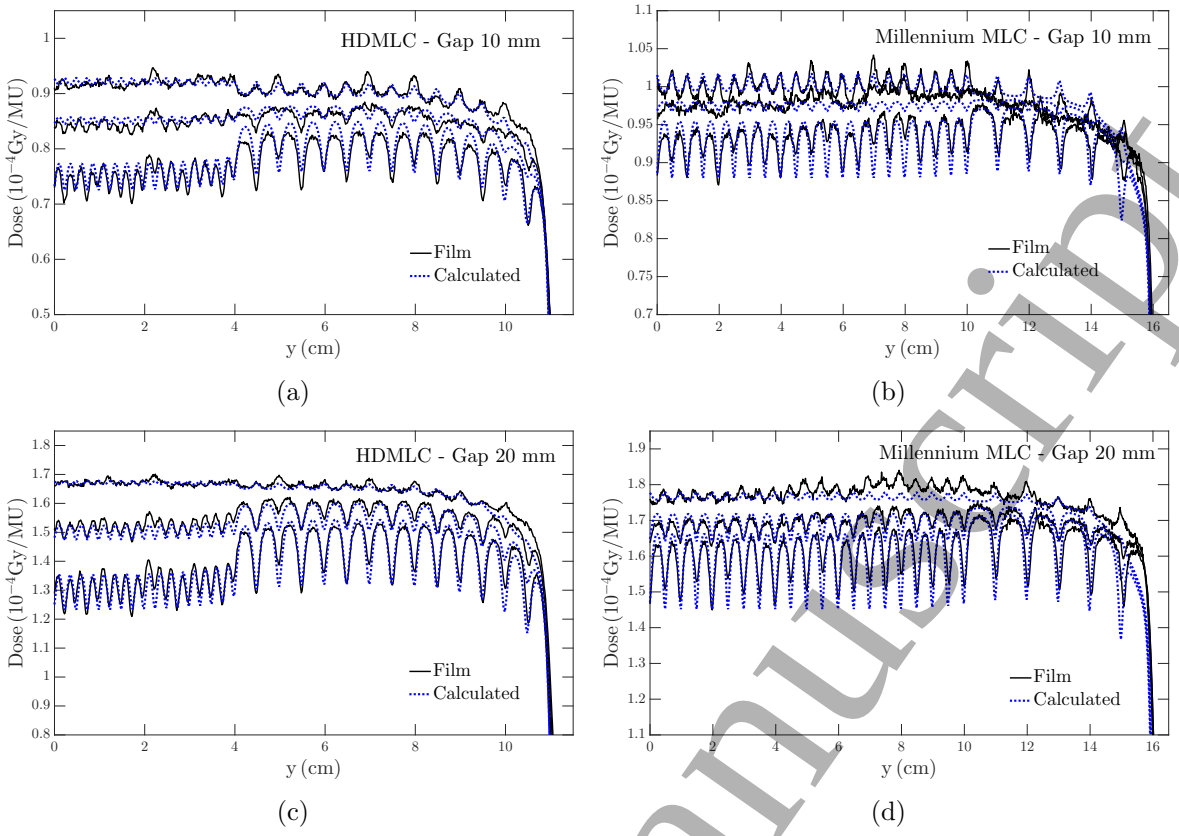

Figure 7: Experimental and calculated profiles obtained for dynamic gaps of 10 mm and 20 mm for the HDMLC (left) and the Millennium MLC (right). In each image three profiles are shown that correspond to different amounts of TG: $s = 0$ (upper), $s =$ 'gap/2' (centre) and $s =$ 'gap' (lower).

of the dose dips (see Fig. 7) for the two MLC models evaluated and for both the central and outer leaves.

4 Discussion

TPSs typically adopt a TG model with a constant TG width and the value of this width determines the slope of the calculated dose curves shown in Fig. 4. Such a model, however, generates big discrepancies in the average doses from asynchronous MLC gaps, notably for small gaps and for the High Definition MLC. In some TPSs this width is a user-definable parameter that can be adjusted to maximise the agreement between calculations and measurements for a reduced set of clinical plans (Chen *et al* 2015). Nevertheless, a constant width model cannot account for the variable slope of the experimental dose curves in Fig. 4 when the exposed length of the tongue s is close to 0 or to the leaf gap. Moreover, we showed that the optimal width depends on the gap size (Fig. 6) and, therefore, there is no single value for the optimal width in a constant

width model. As a consequence, a better modelling of the TG is necessary.

In this study we have presented a method for determining the optimal shape of the TG profile to be subtracted from the fluence map. Our results have a clear physical and geometrical interpretation, because the difference between the experimental $A(s)$ curves illustrated in Fig. 2 and the straight line corresponding to the constant TG width model is due to the rounded leaf end design. As shown in Fig. 1(b), the height of the tongue width is approximately half the leaf height and this is also valid in the rounded leaf tip. Thus, the transmission through the TG width near the leaf tip is not equal to the transmission through the centre of the leaf width and cannot be modelled with the DLG parameter derived from synchronous sweeping gaps. In this study, we have accounted for this effect by using a non-constant TG width, but this effect might be modelled considering a variable transmission below a constant TG width, which would be a more realistic approach. However, using the presented methodology the fluence in the TG region can be obtained with Eq. (11) and this fluence can also be interpreted as the fluence resulting from a constant TG width and a variable transmission. Both approaches, therefore, can be considered equivalent, but the one followed in this study does not require any prior knowledge of the TG width or the MLC geometry.

Regarding the average doses, our model provided calculations in agreement with measurements to within ± 1%. This was true for all gap sizes and amounts of TG effects, while much larger discrepancies were found when a constant TG width was assumed. Although the differences in the $A(s)$ curves shown in Fig. 3 may not seem particularly important, they can explain the experimental discrepancies found. For instance, the difference between the experimentally determined $A(s)$ curve for the HDMLC and the one used by the Eclipse TPS for $s = 5\,\text{mm}$ is approximately $0.5\,\text{mm}^2$, which produces a difference of $1\,\text{mm}^2$ in the area of the asynchronous sweeping gaps when both leaf sides are considered. For a gap size of 5 mm, the exposed area is approximately $12.5\,\text{mm}^2$ (5 mm x 2.5 mm) and $1\,\text{mm}^2$ represents a percentage difference of 8%. For the Millennium MLC the differences in the $A(s)$ curve with respect to the TPS are slightly higher but, since the leaf width is twice as big ($\text{w}_{\text{leaf}} = 5\,\text{mm}$ instead of 2.5 mm), they cause smaller percentage discrepancies.

With respect to the dose distribution, our model accurately reproduced the alternate dose peak-and-valley pattern associated to the TG effect. Two requirements are needed to accurately calculate these details: a fine calculation resolution and modelling of the interleaf transmission. A calculation grid of 1 mm is sufficient for the leaf widths of the Millennium MLC, but a finer calculation grid is needed to accurately sample the peaks and valleys for the central 2.5 mm-wide leaves of the HDMLC (Yang *et al* 2016; Hernandez *et al* 2017). For this reason, we used a higher resolution in this study, with a pixel size of 0.3125 mm. Modelling the interleaf transmission is needed because T_{inter} increases the dose in the region between leaves and, therefore, tends to counteract the TG effect. Thus, if only the average MLC transmission is considered, calculations will tend to overestimate the dose valleys produced by the TG effect and they might even predict dose valleys in situations where there are actually dose peaks due to interleaf transmission dominating over the TG effect (Hernandez *et al* 2017). Despite that, clinical plans use arcs or multiple beams with different orientations and the geometrical

structure of the TG effect is smoothed out in the resulting dose distributions (Deng *et al* 2001). Hence, the fine details of the dose peak-and-valley pattern are not critical in clinical plans and the most clinically relevant quantity is the average dose. Our TG model provides accurate calculations of the average doses even if interleaf transmission is not considered, as long as the dose distribution is properly sampled (Ong *et al* 2011; Yang *et al* 2016).

The impact of this improvement in the MLC modelling will strongly depend on each particular treatment plan. In plans with large MLC gaps and moderate TG effects the differences will be minor, but in plans involving small MLC gaps and irregular MLC apertures the consequences can become clearly noticeable. In Fig. 8 we show an example of calculated and measured dose profiles corresponding to a stereotactic VMAT plan delivered at a fixed gantry and at 10 cm depth (i.e., delivered as a sliding window beam in the same conditions as the rest of the experiments in the present study). As it can be seen, calculations underestimated the delivered dose when a constant TG width was considered (a_2=0), with average dose discrepancies around 2–3%. These discrepancies were confirmed with an ion chamber and were similar to those predicted by the Eclipse TPS. On the other hand, a much better agreement was obtained by using the experimentally determined a_2 parameter, with most dose discrepancies within $\pm$1%. Thus, this refinement in the TG modeling has the potential to improve the calculation accuracy in clinical cases and the corresponding QA results, especially for highly complex plans involving small MLC gaps.

The shape of the optimal TG profile might, in principle, depend on the design of the leaves, on the reproducibility of the MLC manufacturing process, and on the beam quality. The differences found between the two MLC models evaluated can indeed be explained by differences in their design. Thus, the parameter a_1 is very similar for both models because their leaf height and density are also similar (slightly higher for the HDMLC model). On the other hand, the parameter a_2 is much lower for the HDMLC because its leaf curvature radius is twice the radius value of the Millennium MLC (16 cm instead of 8 cm, Fix *et al* 2011), and therefore the curvature correction is smaller. These parameters were determined considering only the central leaves, but film measurements indicate that the parameters found are also valid for the outer leaves. This can be explained because the central and outer leaves have a similar TG design, despite their different widths.

The three MLCs of each model evaluated in this study produced very similar results and could be modelled with a single set of parameters. Hence, a generic solution can be used for each MLC model, avoiding the need for specific measurements and user-definable parameters. This indicates that the MLC manufacturing process is very reproducible and that the parameters used in the model depend little on the photon beam quality. The fact that good agreement was found with the same parameters for the average doses produced by 18 MV x-rays supports this result.

A limitation of this study is that only individual beams were evaluated. Future work will address the impact of using this model in clinical plans with multiple beam orientations and in VMAT treatments. However, we have shown that results in VMAT plans

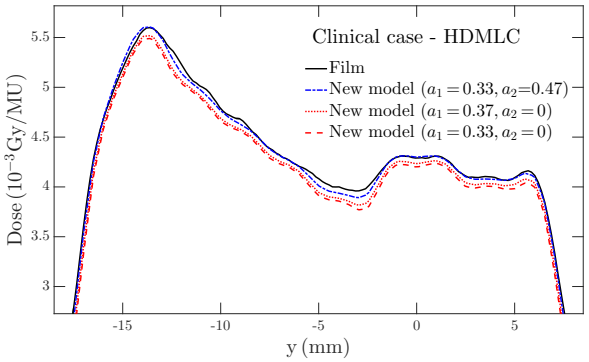

(a)

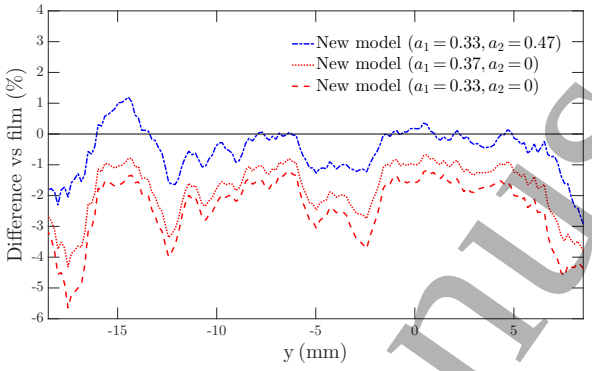

(b)

Figure 8: Experimental and calculated dose profiles in the y axis (perpendicular to the leaf motion) for a clinical plan with the High Definition MLC are shown in (a). The corresponding relative dose differences are given in (b).

were compatible with the results found for individual beams at 10 cm depth (Hernandez *et al* 2017). Another limitation is that only two MLC models were investigated, but the methodology presented is valid regardless of the MLC design and can be applied in general to any MLC. In this study we only evaluated the Eclipse TPS, but most commercial TPSs use similar TG models (Bedford *et al* 2013; Chen *et al* 2015; Roche *et al* 2018) and might benefit from the new model we proposed.

5 Conclusions

A new model for the tongue-and-groove effect and the methodology that derives the required parameters have been presented. This model improves the accuracy of dose calculations whenever leaf sides are included in the exposed beam, notably for MLCs with rounded leaf ends and thin leaf widths (such as Varian's HDMLC). This new model can be easily implemented in commercial TPSs and has the potential to further increase their accuracy in clinical plans.

Acknowledgements

The authors would like to thank Nuria Jornet, from Hospital de la Santa Creu i Sant Pau, for her suggestions and thoughtful comments. This method is currently in patent pending status.

References

Azcona J and Burguete J 2010 Intensity modulated dose calculation with an improved experimental pencil-beam kernel *Medical Physics 9*(37) 4634–4642

Bedford J L, Thomas M D and Smyth G 2013 Beam modeling and vmat performance with the agility 160-leaf multileaf collimator *Journal of applied clinical medical physics 14*(2) 172–185

Chen S, Yi B Y, Yang X, Xu H, Prado K L and D'Souza W D 2015 Optimizing the MLC model parameters for IMRT in the RayStation treatment planning system *Journal of Applied Clinical Medical Physics 16*(5) 322–332

Chui C S, LoSasso T and Palm A 2003 *A practical guide to intensity modulated radiation therapy, chapter 4* Madison, WI: Medical Physics Publishing

Deng J, Pawlicki T, Chen Y, Li J, Jiang S B and Ma C M 2001 The MLC tongue-and-groove effect on IMRT dose distributions. *Physics in Medicine & Biology 46*(4) 1039–60

Fix M K, Volken W, Frei D, Frauchiger D, Born E J and Manser P 2011 Monte Carlo implementation, validation, and characterization of a 120 leaf MLC. *Medical physics 38*(10) 5311–20

Hernandez V, Sanchez-Vera J A, Vieillevigne L and Saez J 2017 Commissioning of the tongue-and-groove modelling in treatment planning systems: from static fields to VMAT treatments *Physics in medicine and biology* (62) 6688–6707

Hillman Y, Kim J, Chetty I and Wen N 2018 Refinement of mlc modeling improves commercial qa dosimetry system for srs and sbrt patient-specific qa *Medical Physics 45*(4) 1351–1359

Li J S, Lin T, Chen L, Price R a and Ma C M 2010 Uncertainties in IMRT dosimetry. *Medical physics 37*(May) 2491–2500

Lorenz F, Nalichowski A, Rosca F, Killoran J, Wenz F and Zygmanski P 2008 An independent dose calculation algorithm for MLC-based radiotherapy including the spatial dependence of MLC transmission. *Physics in medicine and biology 53*(3) 557–573

LoSasso T, Chui C and Ling C 1998 Physical and dosimetric aspects of a multileaf collimation system used in the dynamic mode for implementing intensity modulated radiotherapy. *Medical physics 25*(10) 1919–1927

Mans A, Schuring D, Arends M P, Vugts C A J M, Wolthaus J W H, Lotz H T, Admiraal M, Louwe R J W, Öllers M C and van de Kamer J B 2016 The NCS code of practice for the quality assurance and control for volumetric modulated arc therapy. *Physics in medicine and biology 61*(19) 7221–7235

Mei X, Nygren I and Villarreal-Barajas J E 2011 On the use of the MLC dosimetric leaf gap as a quality control tool for accurate dynamic IMRT delivery. *Medical physics 38*(4) 2246–2255

Ong C L, Cuijpers J P, Senan S, Slotman B J and Verbakel W F A R 2011 Impact of the calculation resolution of AAA for small fields and RapidArc treatment plans. *Medical Physics 38*(8) 4471–9

Roche M, Crane R, Powers M and Crabtree T 2018 Agility mlc transmission optimization in the monaco treatment planning system *Journal of Applied Clinical Medical Physics 19*(5) 473–482

Tillikainen L, Siljamaki S, Helminen H, Alakuijala J and Pyyry J 2007 Determination of parameters for a multiple-source model of megavoltage photon beams using optimization methods *Physics in medicine and biology 5*(52) 1441–1467

Torsti T, Korhonen L and Medical V 2013 Using Varian Photon Beam Source Model for Dose Calculation of Small Fields (September)

Varian Medical Systems 2015 Eclipse Photon and Electron Reference Guide pp. 263–348

Yang J, Tang G, Zhang P, Hunt M, Lim S B, LoSasso T and Mageras G 2016 Dose calculation for hypofractionated volumetric-modulated arc therapy: Approximating continuous arc delivery and tongue-and-groove modeling *Journal of Applied Clinical Medical Physics 17*(2) 3–13